

# Two Novel Glycoside Hydrolases Responsible for the Catabolism of Cyclobis-(1→6)- $\alpha$ -nigerosyl\*

Received for publication, March 14, 2016, and in revised form, June 6, 2016. Published, JBC Papers in Press, June 14, 2016, DOI 10.1074/jbc.M116.727305

Takayoshi Tagami<sup>†1</sup>, Eri Miyano<sup>‡</sup>, Juri Sadahiro<sup>‡</sup>, Masayuki Okuyama<sup>‡</sup>, Tomohito Iwasaki<sup>‡</sup>, and Atsuo Kimura<sup>§2</sup>

From the <sup>†</sup>College of Agriculture, Food and Environment Sciences, Rakuno Gakuen University, Ebetsu 069-8501 and the <sup>‡</sup>Research Faculty of Agriculture, Hokkaido University, Sapporo 060-8589, Japan

The actinobacterium *Kribbella flavida* NBRC 14399<sup>T</sup> produces cyclobis-(1→6)- $\alpha$ -nigerosyl (CNN), a cyclic glucotetraose with alternate  $\alpha$ -(1→6)- and  $\alpha$ -(1→3)-glucosidic linkages, from starch in the culture medium. We identified gene clusters associated with the production and intracellular catabolism of CNN in the *K. flavida* genome. One cluster encodes 6- $\alpha$ -glucosyltransferase and 3- $\alpha$ -isomaltosyltransferase, which are known to coproduce CNN from starch. The other cluster contains four genes annotated as a transcriptional regulator, sugar transporter, glycoside hydrolase family (GH) 31 protein (Kfla1895), and GH15 protein (Kfla1896). Kfla1895 hydrolyzed the  $\alpha$ -(1→3)-glucosidic linkages of CNN and produced isomaltose via a possible linear tetrasaccharide. The initial rate of hydrolysis of CNN (11.6 s<sup>-1</sup>) was much higher than that of panose (0.242 s<sup>-1</sup>), and hydrolysis of isomaltotriose and nigerose was extremely low. Because Kfla1895 has a strong preference for the  $\alpha$ -(1→3)-isomaltosyl moiety and effectively hydrolyzes the  $\alpha$ -(1→3)-glucosidic linkage, it should be termed 1,3- $\alpha$ -isomaltosidase. Kfla1896 effectively hydrolyzed isomaltose with liberation of  $\beta$ -glucose, but displayed low or no activity toward CNN and the general GH15 enzyme substrates such as maltose, soluble starch, or dextran. The  $k_{cat}/K_m$  for isomaltose (4.81  $\pm$  0.18 s<sup>-1</sup> mM<sup>-1</sup>) was 6.9- and 19-fold higher than those for panose and isomaltotriose, respectively. These results indicate that Kfla1896 is a new GH15 enzyme with high substrate specificity for isomaltose, suggesting the enzyme should be designated an isomaltose glucohydrolase. This is the first report to identify a starch-utilization pathway that proceeds via CNN.

Cyclobis-(1→6)- $\alpha$ -nigerosyl (CNN),<sup>3</sup> also known as cycloalternan or cyclic tetrasaccharide, is a cyclic glucotetraose with alternate  $\alpha$ -(1→6)- and  $\alpha$ -(1→3)-glucosidic linkages (Fig. 1). This cyclic sugar was first produced from alternan, an alternating linear  $\alpha$ -(1→6)-/ $\alpha$ -(1→3)-glucan, by treatment with a

glycanase termed alternanase, which is produced by *Bacillus* sp. NRRL B-21195 (1). Nishimoto and co-workers (2–4) subsequently identified three bacterial species (*Sporosarcina globisporpora* C11 and N75, formerly known as *Bacillus globisporus*, and *Arthrobacter globiformis* A19) that generate CNN from starch. Their ability to produce CNN is derived from two extracellular glycosyltransferases: 6- $\alpha$ -glucosyltransferase (6-GT) and 3- $\alpha$ -isomaltosyltransferase (IMT). 6-GT catalyzes  $\alpha$ -(1→6)-glucosyl transfer to the nonreducing terminal glucose unit of  $\alpha$ -(1→4)-glucan (GLn) and produces  $\alpha$ -glucosyl-(1→6)-GLn ( $\alpha$ -isomaltosyl-GLn). IMT utilizes  $\alpha$ -isomaltosyl-GLn as both donor and acceptor substrate and catalyzes the  $\alpha$ -(1→3) transfer of the  $\alpha$ -isomaltosyl moiety of one substrate to the other, resulting in  $\alpha$ -isomaltosyl-(1→3)- $\alpha$ -isomaltosyl-GLn formation. Furthermore, IMT catalyzes the intramolecular cyclization of  $\alpha$ -isomaltosyl-(1→3)- $\alpha$ -isomaltosyl-GLn, and eventually generates CNN. Currently, it is known that *Bacillus* sp. NRRL B-21195 produces CNN from maltooligosaccharides using the alternanase and a 6-GT (5, 6). Gene clusters encoding 6-GT and IMT were identified in *S. globisporpora* C11 and N75, and *A. globiformis* A19 (3, 4, 7). Their 6-GT and IMT share high sequence similarity with related enzymes found among the bacterial species. All these enzymes are members of glycoside hydrolase family (GH) 31, which is a sequence-based enzyme classification (8). These studies imply that a common starch metabolic pathway that proceeds via CNN, in which 6-GT and IMT play crucial roles, had been distributed in some bacterial species beyond the genus.

Although CNN-producing enzymes have been identified in some bacteria, whether and how the bacterial species utilize CNN as a carbon source is unclear. Kim *et al.* (9) reported the purification and characterization of a CNN-degrading enzyme from a lysate of *Bacillus* sp. NRRL B-21195. This intracellular enzyme hydrolyzed CNN and produced isomaltose via the intermediate  $\alpha$ -isomaltosyl-(1→3)-isomaltose. Thus, the authors suggested that CNN is imported into the cells in its cyclic form, as well as cyclomaltodextrins, which are the most widely known cyclic glucans (10). However, the complete CNN degradation pathway is yet unclear because no gene encoding a CNN-degrading enzyme or related proteins, such as a transporter or an isomaltose-degrading enzyme, has been identified.

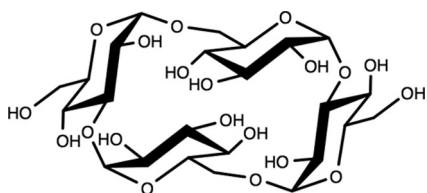
In the present study, we revealed that the actinobacterium *Kribbella flavida* NBRC 14399<sup>T</sup> extracellularly produces CNN from starch, and intracellularly degrades CNN into glucose via isomaltose. *K. flavida* is a Gram-positive, aerobic, and mesophilic actinomycete isolated from soil or scabby potato, and its genome has been completely sequenced (11). This enabled us to

\* This work was supported in part by Grants-in-Aid for Regional R&D Proposal-based Program from Northern Advancement Center for Science & Technology of Hokkaido Japan. The authors declare that they have no conflicts of interest with the contents of this article.

<sup>1</sup> To whom correspondence may be addressed: Rakuno Gakuen University, 582, Bunkyo-dai-Midorimachi, Ebetsu 069-8501, Japan. Tel./Fax: 81-11-388-4603; E-mail: t-tagami@rakuno.ac.jp.

<sup>2</sup> To whom correspondence may be addressed: Research Faculty of Agriculture, Hokkaido University, Kita-9 Nishi-9, Kita-ku, Sapporo 060-8589, Japan. Tel./Fax: 81-11-706-2808; E-mail: kimura@abs.agr.hokudai.ac.jp.

<sup>3</sup> The abbreviations used are: CNN, cyclobis-(1→6)- $\alpha$ -nigerosyl; 6-GT, 6- $\alpha$ -glucosyltransferase; ABC, ATP-binding cassette; ESI, electrospray ionization; GH, glycoside hydrolase family; GLn,  $\alpha$ -(1→4)-glucan; IMT, 3- $\alpha$ -isomaltosyltransferase; ROK, repressor open reading frame kinase.

FIGURE 1. Cyclobis-(1→6)- $\alpha$ -nigerosyl.

identify two gene clusters related to CNN production and CNN degradation, respectively, in the genome. CNN degradation is catalyzed by two novel glycoside hydrolases that belong to GH31 and GH15, respectively. This is the first report to demonstrate this unique pathway, which metabolizes starch to glucose via CNN.

## Results

**Production and Degradation of CNN by *K. flavida***—*K. flavida* was cultured using soluble starch as the sole carbon source. The bacterium accumulated some oligosaccharides in the culture supernatant, one of which was a glucoamylase-resistant carbohydrate (Fig. 2A). Its molecular weight was estimated to be 648.2 using electrospray ionization (ESI)-MS analysis, and all chemical shifts observed in the  $^1\text{H}$  and  $^{13}\text{C}$  NMR spectra corresponded to those of CNN (1) (data not shown). These results demonstrate that this oligosaccharide was CNN.

The time courses of growth ( $A_{600}$ ) and CNN concentration in the culture supernatant were monitored (Fig. 2B). The  $A_{600}$  increased during the first 72 h of cultivation and then was decreased upon further cultivation. CNN was not observed in the culture medium until 72 h of cultivation, but further cultivation increased the accumulation of CNN. These observations indicate that *K. flavida* accumulated CNN in the death phase. The carbohydrate assimilation test showed that *K. flavida* grew well on CNN at the same level as on glucose and maltose (Fig. 2C), meaning that CNN is a favorable carbon source for this bacterium.

To ascertain whether *K. flavida* possesses CNN-degrading activity, a cell-free lysate, and a membrane fraction were reacted on CNN (Fig. 2D). Although the membrane fraction did not degrade CNN, the cell-free lysate produced isomaltose, glucose, and an oligosaccharide that may be a linearized CNN. This result indicates that *K. flavida* intracellularly catabolizes CNN via isomaltose.

**Candidate Gene Clusters Related to the Production and Degradation of CNN**—A search for genes in the *K. flavida* genome that encode proteins sharing similarity with IMT of *A. globiformis* A19 (UniProtKB accession: Q6BD67) was performed using the protein BLAST. Based upon the search results, we focused on two genetic loci: *Kfla\_4052* and *Kfla\_1895*.

*Kfla\_4052* appears to form a gene cluster with *Kfla\_4051* and *Kfla\_4053* (Fig. 3A). The 1,108-amino acid GH31 protein encoded by *Kfla\_4052*, designated Kfla4052, shares 79.0% similarity (with 0.4% gaps; calculated using the EMBOSS Water pairwise sequence alignment tool (12)) with the IMT of *A. globiformis* A19. The 948-amino acid protein encoded by *Kfla\_4051*, designated Kfla4051, shares high (78.3%) sequence similarity with the GH31 protein 6-GT of *A. globiformis* A19. The upstream gene (*Kfla\_4053*) was annotated as encoding a

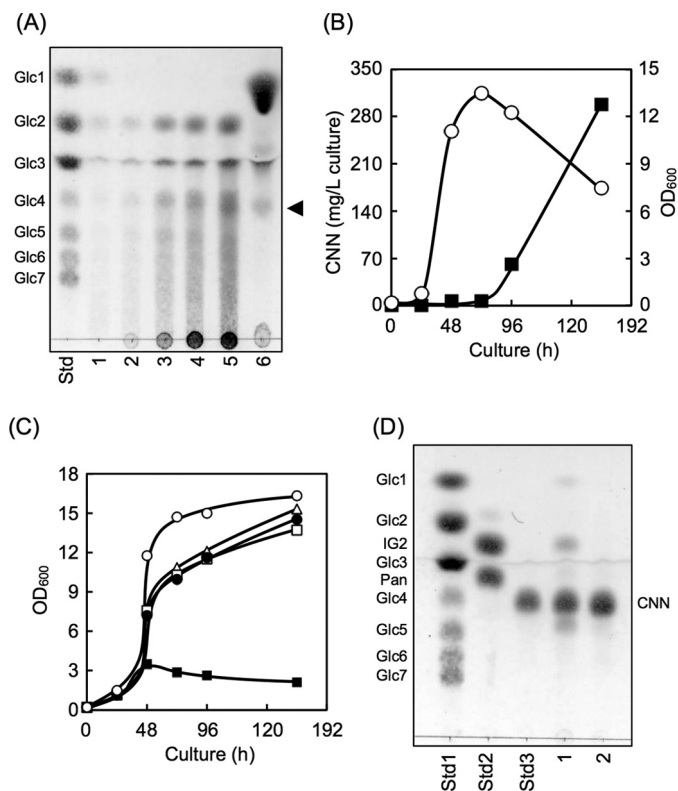
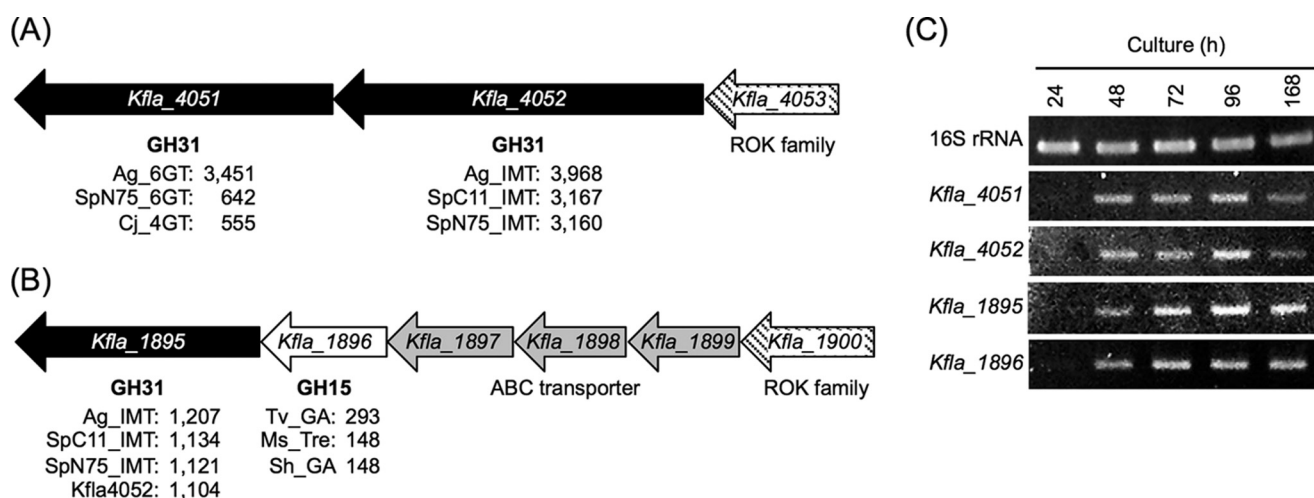


FIGURE 2. Production and degradation of CNN by *K. flavida* NBRC 14399<sup>T</sup>. A, TLC analysis of the soluble carbohydrates remaining after 80% ethanol precipitation of the culture supernatant during CNN production. Lane Std, glucose (Glc1) and a series of maltooligosaccharides from maltose (Glc2) to maltoheptaose (Glc7); lanes 1–5, culture supernatant obtained after 24, 48, 72, 96, and 168 h of culture, respectively; lane 6, glucoamylase-treated 168-h culture supernatant. The arrowhead indicates CNN. B, growth curve (circle) and CNN concentration (square) during cultivation in CNN-producing medium. C, growth curves during cultivation in 5% various carbon sources. Closed square, without carbon source; triangle, glucose; open square, maltose; closed circle, CNN; open circle, soluble starch. D, TLC analysis of the reaction mixtures of CNN with the cell-free lysate or the membrane fraction of *K. flavida* NBRC 14399<sup>T</sup>. Lane Std1, Glc1–Glc7; lane Std2, isomaltose (IG2) and panose (Pan); lane Std3, CNN; lanes 1 and 2, reaction mixture with the cell-free lysate or the membrane fraction, respectively.

transcriptional regulator: repressor, open reading frame, kinase (ROK) family protein. Both Kfla4051 and Kfla4052 were predicted to possess a signal peptide, indicating that they are extracellular enzymes.

*Kfla\_1895* appears to form another gene cluster with *Kfla\_1896* to *Kfla\_1900* (Fig. 3B). The 723-amino acid GH31 protein encoded by *Kfla\_1895*, designated Kfla1895, shares similarities with the IMT of *A. globiformis* A19 (46.2% similarity with 17.3% gaps) as well as other IMTs and Kfla4052. These enzymes were predicted to have an extra domain, a family-35 carbohydrate-binding module (CBM35) (8), at the C-terminal side of the catalytic domain, whereas Kfla1895 was predicted to be a single-domain protein. Its upstream gene, *Kfla\_1896*, was annotated as encoding a family-15 glycoside hydrolase. However, this 385-amino acid enzyme, Kfla1896, shared very weak similarity with GH15 enzymes, such as the glucoamylase of *Thermoactinomyces vulgaris* R-47 (37.1%) and the  $\alpha$ , $\alpha$ -trehalase of *Mycobacterium smegmatis* str. MC2 155 (37.6%) because of high gap scores (25.2 and 15.4%, respectively). Both Kfla1895 and Kfla1896 were predicted to be intracellular pro-

## Two Novel Glycosidases of GH31 and GH15 Degrade CNN



**FIGURE 3. Analysis of candidate genes.** A and B, two focused gene clusters containing *Kfla\_4052* and *Kfla\_1895*, respectively. The values below each gene indicate the pairwise alignment score calculated using EMBOSS Water (12). The enzyme abbreviations and their UniProtKB accessions as follows: Ag\_6GT, 6-GT of *A. globiformis* A19 (Q6BD65); SpN75\_6GT, 6-GT of *S. globispora* N75 (Q84IQ2); Cj\_4GT, oligosaccharide  $\alpha$ -1,4-transglucosylase of *Cellvibrio japonicus* Ueda107 (B3PEE6); Ag\_IMT, IMT of *A. globiformis* A19 (Q6BD67); SpC11\_IMT, IMT of *S. globispora* C11 (Q8RQV0); SpN75\_IMT, IMT of *S. globispora* N75 (Q84IQ3); Tv\_GA, glucoamylase of *T. vulgaris* R-47 (Q9KWR2); Ms\_Tre,  $\alpha$ , $\alpha$ -trehalase of *M. smegmatis* str. MC2 155 (A0R0W9); Sh\_GA, glucoamylase of *Streptomyces hygroscopicus* subsp. *limoneus* KCCM 11405 (Q15JF7). C, gene expression analysis by semiquantitative RT-PCR. The 16S rRNA encoded by *Kfla\_R0040* was used as a reference gene.

teins because there was no possible signal peptide. Putative genes encoding a sugar ATP-binding cassette (ABC) transporter and an ROK family protein exist in their upstream regions.

The expression levels of *Kfla\_4051*, *4052*, *1895*, and *1896* in *K. flavigida* cells during CNN production were analyzed by semiquantitative RT-PCR (Fig. 3C). All of their transcripts were present at detectable levels in cells cultured for 48 h or more. The expression levels of *Kfla\_1895* and *Kfla\_1896* were maintained during 168 h of culture, but those of *Kfla\_4051* and *Kfla\_4052* decreased at 168 h compared with their levels from 48 to 96 h.

**Enzymatic Properties of *Kfla4052*, *Kfla1895*, and *Kfla1896***—*Kfla4051*, *Kfla4052*, *Kfla1895*, and *Kfla1896* were expressed as recombinant proteins in *Escherichia coli*. All of the recombinant enzymes, except *Kfla4051*, were produced in a soluble form. *Kfla4052*, *Kfla1895*, and *Kfla1896* were purified and characterized.

*Kfla4052* was reacted on 20 mM panose ( $\alpha$ -isomaltosyl-(1 $\rightarrow$ 4)-glucose) and the products were analyzed using TLC (Fig. 4A). The enzyme initially produced glucose and an oligosaccharide with a retention factor similar to that of maltohexaose. Subsequently, the reaction mixture accumulated CNN, indicating that *Kfla4052* is a typical IMT. The oligosaccharide should be  $\alpha$ -isomaltosyl-(1 $\rightarrow$ 3)- $\alpha$ -isomaltosyl-(1 $\rightarrow$ 4)-glucose. The activity of *Kfla4052*, defined using the rate of glucose release from 10 mM panose, was enhanced 18-fold in the presence of 1 mM  $\text{CaCl}_2$ . The activity was the highest at pH 6.6, and the enzyme was stable at pH 3.2–10.1 and at  $<55^\circ\text{C}$ .

*Kfla1895* was reacted on 10 mM CNN and the products were analyzed using TLC (Fig. 4B, lanes 1–5). The enzyme initially produced a possible linearized CNN (its spot appears under that of CNN) and subsequently accumulated isomaltose. The initial rate for hydrolysis of 10 mM CNN, determined by an increase in the concentration of reducing ends, was  $11.6\text{ s}^{-1}$ . *Kfla1895* activity was the highest at pH 7.9, and the enzyme was

stable between pH 6.8 and at least pH 10.7, and at  $<41^\circ\text{C}$ . *Kfla1895* also hydrolyzed panose into glucose and isomaltose (data not shown); however, the initial rate of panose hydrolysis was 2% of that of CNN, and those of isomaltotriose and nigerose were vanishingly low (Table 1). The  $s$ - $v$  plots for the hydrolysis of CNN were fitted to the Michaelis-Menten equation (Fig. 4C) and the  $k_{\text{cat}}$  and  $K_m$  values were determined to be  $22.3 \pm 1.7\text{ s}^{-1}$  and  $7.63 \pm 1.38\text{ mM}$ , respectively. The  $k_{\text{cat}}/K_m$  for CNN ( $2.97 \pm 0.34\text{ s}^{-1}\text{ mM}^{-1}$ ) was 57-fold higher than for panose (Table 2). The sequence comparison with other GH31 enzymes revealed that two conserved regions, regions A and B, including the catalytic nucleophile and acid/base Asp residues, respectively (13), were also observed in *Kfla1895* (Fig. 5A). The site-directed mutations of Asp<sup>451</sup> and Asp<sup>516</sup> of *Kfla1895* to Ala resulted in complete loss of the CNN hydrolyzing activity (Fig. 5B). These results implied that Asp<sup>451</sup> and Asp<sup>516</sup> of *Kfla1895* were, respectively, catalytic nucleophile and acid/base as found for other GH31 enzymes.

*Kfla1896* was reacted on the reaction products from *Kfla1895*-catalyzed CNN hydrolysis, and the products of this reaction were analyzed using TLC (Fig. 4B, lanes 6 and 7). *Kfla1896* completely hydrolyzed isomaltose to glucose and generated another oligosaccharide having a retention value similar to that of panose. Substrate specificity analysis revealed that *Kfla1896* displays the highest reaction rate with isomaltose, lower rates with panose and isomaltotriose, but almost no activity with other  $\alpha$ -glucobioses (trehalose, kojibiose, nigerose, and maltose), CNN, or polysaccharides (dextran and soluble starch) (Table 1). The isomaltose-hydrolyzing activity was the highest at pH 6.7, and the enzyme was stable between pH 6.5 and at least pH 11.2, and at  $<35^\circ\text{C}$ . All  $s$ - $v$  plots for the hydrolysis of isomaltose, panose, and isomaltotriose were fitted to the Michaelis-Menten equation (Fig. 4D) and their kinetic parameters were determined (Table 2). *Kfla1896* displayed a  $K_m$  value for isomaltose that was similar to those of its other substrates, but a 10-fold higher  $k_{\text{cat}}$  value for isomaltose than those

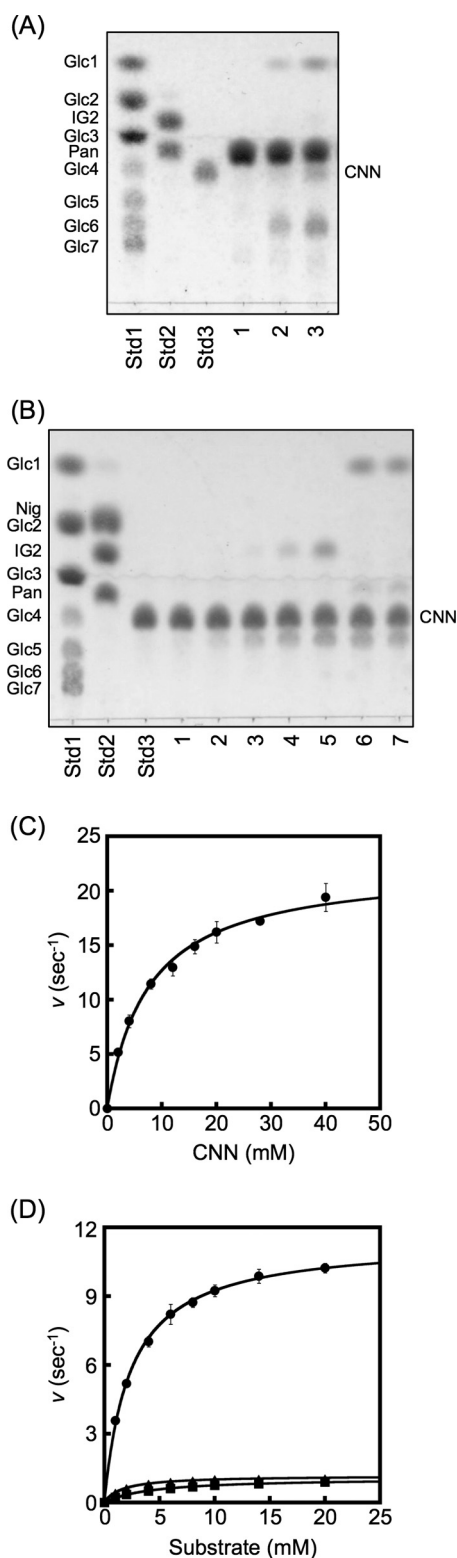


FIGURE 4. Characterization of Kfla4052, Kfla1895, and Kfla1896. *A*, Kfla4052-catalyzed CNN production from panose. TLC analysis was performed using a reaction mixture containing Kfla4052 (0.16 units/ml) and panose (20 mM). Lanes *Std1–Std3*, same as described in the legend to Fig. 2*D*; lanes 1–3, the reaction mixture at 0, 5, and 15 min, respectively. *B*, CNN degradation to glucose by Kfla1895 and Kfla1896. TLC analysis was done using the reaction mixture of Kfla1895 (0.011 units/ml) with CNN (10 mM) (lanes 1–5) and that of Kfla1896 (0.85 units/ml) with the resultant 240 min-reaction mixture of Kfla1895 and CNN (lanes 6 and 7). Lanes *Std1–Std3*, the same as in Fig. 2*D*, except *Std2* that contains nigerose (*Nig*); lanes 1–5, the reaction mixture at 10, 30, 60, 120, and 240 min, respectively; lanes 6 and 7, the reaction mixture at

TABLE 1  
Substrate specificities of Kfla1895 and Kfla1896

Substrate	$v$	Ratio of $v$
	$s^{-1}$	%
<b>Kfla1895</b>		
CNN	11.6	100
Panose	$2.42 \times 10^{-1}$	2.1
Isomaltotriose	$1.01 \times 10^{-3}$	0.0087
Nigerose	$9.90 \times 10^{-3}$	0.085
<b>Kfla1896</b>		
Isomaltose	8.58	100
Panose	$9.93 \times 10^{-1}$	12
Isomaltotriose	$6.75 \times 10^{-1}$	7.9
Dextran 10	$4.09 \times 10^{-2}$	0.48
Trehalose	$9.80 \times 10^{-3}$	0.11
Kojibiose	$3.90 \times 10^{-3}$	0.046
Nigerose	$4.76 \times 10^{-4}$	0.0055
Maltose	$4.76 \times 10^{-4}$	0.0055
Soluble starch	$9.52 \times 10^{-4}$	0.011
CNN	$<7.09 \times 10^{-4}$	$<0.0083$

TABLE 2  
Kinetic parameters of Kfla1895 and Kfla1896

Substrate	$k_{cat}$	$K_m$	$k_{cat}/K_m$
	$s^{-1}$	mM	$s^{-1} mM^{-1}$
<b>Kfla1895</b>			
CNN	$22.3 \pm 1.7$	$7.63 \pm 1.38$	$2.97 \pm 0.34$
Panose	ND <sup>a</sup>	ND	$0.0524 \pm 0.0086$
<b>Kfla1896</b>			
Isomaltose	$11.4 \pm 0.3$	$2.38 \pm 0.07$	$4.81 \pm 0.18$
Panose	$1.17 \pm 0.01$	$1.68 \pm 0.06$	$0.699 \pm 0.020$
Isomaltotriose	$1.07 \pm 0.02$	$4.36 \pm 0.21$	$0.247 \pm 0.008$

<sup>a</sup> ND, not determined.

for the other substrates. Thus, Kfla1896 exhibited a  $k_{cat}/K_m$  value for isomaltose that was 6.9- and 19-fold higher than those for panose and isomaltotriose, respectively. The anomeric configuration analysis of product showed that Kfla1896 produced the  $\beta$ -anomer of glucose (data not shown). Furthermore, Kfla1896 possessed two conserved regions among GH15 enzymes, regions III and V, including the catalytic acid and base glutamic acid residues, respectively (14), and the substitutions of Glu<sup>178</sup> and Glu<sup>335</sup> of Kfla1896 by Ala markedly decreased or lost the activity (Fig. 5, *C* and *D*). These results indicated that the catalytic mechanism of Kfla1896 is identical to those of other GH15 enzymes.

## Discussion

Although an enzyme system that produces CNN from starch was found in some bacterial species two decades ago, it had not been clear how these microorganisms use CNN as a carbon source. The present study demonstrated that *K. flavida* NBRC 14399<sup>T</sup> produces CNN extracellularly from starch and degrades CNN intracellularly to glucose. The proteins involved in the metabolic pathway are encoded by two gene clusters, from *Kfla\_4051* to *Kfla\_4053* for production, and from *Kfla\_1895* to *Kfla\_1900* for catabolism. Each gene cluster is likely to be regulated by its own ROK family protein, encoded by *Kfla\_4053* or *Kfla\_1900*, respectively. ROK family proteins are often found as transcriptional repressors for sugar catabolic operons (15). CNN production from starch may be catalyzed by

22 h and 3 days, respectively. *C*,  $s$ - $v$  plots of Kfla1895 for CNN. *D*,  $s$ - $v$  plots of Kfla1896. The substrates are isomaltose (circle), panose (triangle), and isomaltotriose (square).

## Two Novel Glycosidases of GH31 and GH15 Degrade CNN

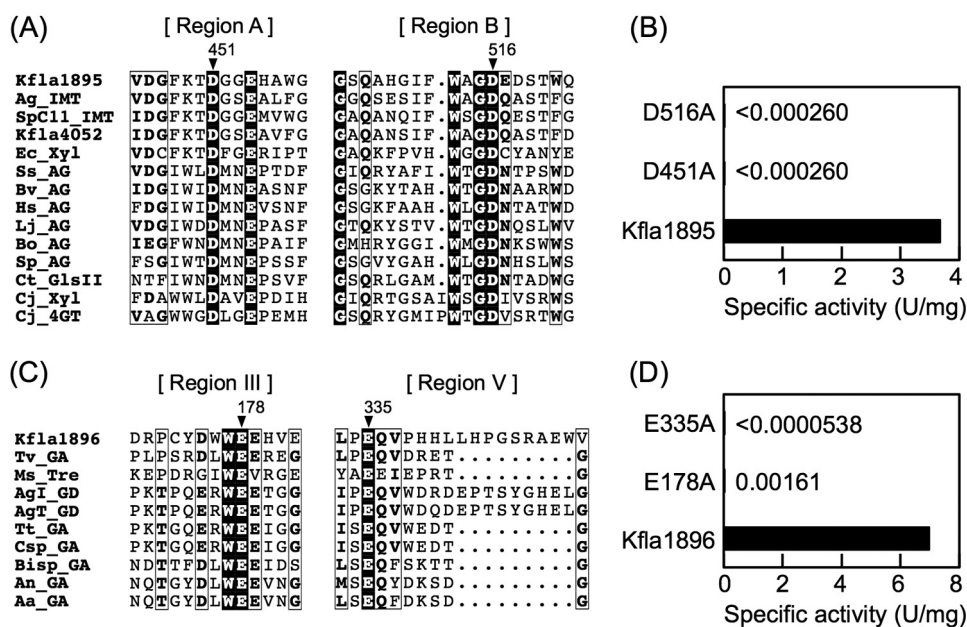


**FIGURE 5. Catalytic residues of Kfla1895 and Kfla1896.** A, multiple sequence alignment around conserved regions A and B in GH31. Asp<sup>451</sup> and Asp<sup>516</sup> in Kfla1895 were predicted as nucleophile and acid/base residues, respectively. The enzyme abbreviations and their UniProtKB accessions are shown in Fig. 3 and also as follows: Ec\_Xyl, *E. coli* str. K-12 substr. MG1655  $\alpha$ -xylosidase (P31434); Ss\_AG, *Sulfolobus solfataricus* 98/2  $\alpha$ -glucosidase (POCD66); Bv\_AG, *Beta vulgaris*  $\alpha$ -glucosidase (O04931); Hs\_AG, *Homo sapiens* maltase unit (O43451); Lj\_AG, *Lactobacillus johnsonii* NBRC 13952  $\alpha$ -1,3-glucosidase (C1KIT5); Bo\_AG, *Blautia obeum* ATCC 29174 (A5ZY13); Sp\_AG, *Schizosaccharomyces pombe* 972h- $\alpha$ -glucosidase (Q9C0Y4); Ct\_GlsII, *Chaetomium thermophilum* var. *thermophilum* DSM 1495 glucosidase II  $\alpha$ -subunit (G0SG42); Cj\_Xyl, *C. japonicus* Ueda107  $\alpha$ -xylosidase (B3PBD9); Cj\_4GT, *C. japonicus* Ueda107 oligosaccharide  $\alpha$ -1,4-transglucosylase (Q8RDL1). B, specific activities of Kfla1895 and its mutant enzymes (D451A and D516A), in which Asp<sup>451</sup> and Asp<sup>516</sup> were substituted by Ala, respectively. C, multiple sequence alignment around conserved regions III and V in GH15. Glu<sup>178</sup> and Glu<sup>335</sup> in Kfla1896 were predicted as acid and base catalytic residues, respectively. The enzyme abbreviations and their UniProtKB accessions are shown in Fig. 3 and also as follows: AgI\_GD, *A. globiformis* I42 glucodextranase (Q9LBQ9); AgT\_GD, *A. globiformis* T-3044 glucodextranase (P70745); Tt\_GA, *Thermoanaerobacterium thermosaccharolyticum* ATCC 7956 glucoamylase (O85672); Csp\_GA, *Clostridium* sp. G0005 glucoamylase (P29761); Bisp\_GA, *Bispora* sp. MEY-1 glucoamylase (GenBank ID AIQ80993); An\_GA, *A. niger* CBS 513.88 glucoamylase (A2QHE1); Aa\_GA, *Aspergillus awamori* X-100 glucoamylase (Q12537). D, specific activities of Kfla1896 and its mutant enzymes (E178A and E335A), in which Glu<sup>178</sup> and Glu<sup>335</sup> were substituted by Ala, respectively. Both multiple sequence alignments were produced using COBALT (33) and rendered using ESPript 3.0 (25).

Kfla4052, with possible assistance from Kfla4051. We showed that Kfla4052 produces CNN from panose, demonstrating that this enzyme is a typical IMT (Fig. 4A). We were unable to produce Kfla4051 in our study, but sequence comparison strongly supports that Kfla4051 is a 6-GT. These findings suggest that *K. flavida* NBRC 14399<sup>T</sup>, as well as other bacterial species, produce CNN from starch using the well known enzyme system consisting of 6-GT and IMT. The extracellularly produced CNN is thought to be imported into the cells via the sugar ABC transporter encoded by *Kfla\_1897-1899* and degraded into glucose by Kfla1895 and Kfla1896. It is proposed that Kfla1895 first degrades CNN into isomaltose and that Kfla1896 subsequently hydrolyzes isomaltose into glucose. The *in vitro* degradation of CNN by Kfla1895 and Kfla1896 corresponded to the degradation that occurred in the cell lysate (Figs. 2D and 4B). This observation supports the hypothesis that Kfla1895 and Kfla1896 are a practical pathway for CNN degradation *in vivo*. This is the first report identifying an enzyme system that catabolizes CNN. The expression levels of the key enzymes that produce and degrade CNN were increased during log-phase growth (Fig. 3C), and CNN did not accumulate at this time (Fig. 2B). These results imply that the utilization of starch via CNN plays a key role in energy production in *K. flavida* NBRC 14399<sup>T</sup>. This bacterium effectively utilizes CNN as carbon source as well as glucose and maltose (Fig. 2C). It is speculated that *K. flavida* produces CNN from starch to secure the carbon

source from competitors. Few bacterial species utilizing CNN have been reported so far. On the other hand, gene clusters containing an ROK-family protein, a sugar ABC transporter, a Kfla1895-like protein, and a Kfla1896-like protein are found in the genomes of *Nocardioideis* sp. JS614 (gene loci: *Noca\_4630–Noca\_4635*), *Microbispora* sp. ATCC PTA-5024 (gene loci: *MPTA5024\_20930–MPTA5024\_20955*), *Intrasporangium oryzae* NRRL B-24470 (gene loci: *N865\_RS16840–N865\_RS16865*), and *Trueperella pyogenes* TP8 (gene loci: *X956\_02355–X956\_02380*), even though the Kfla1896-like protein is replaced with an  $\alpha$ -glucosidase and an oligo-1,6-glucosidase in *I. oryzae* and *T. pyogenes*, respectively. These bacterial species are expected to catabolize CNN according to the same pathway as *K. flavida*. Furthermore, Kim *et al.* (9) previously reported a CNN-degrading enzyme that had no sequence similarity to GH31 enzymes and displayed similar  $k_{cat}/K_m$  values for CNN and panose. This study suggests that another CNN degradation pathway, catalyzed by an enzyme having substrate specificity different from that of Kfla1895, is distributed among the other bacterial species.

The characterizations of Kfla1895 and Kfla1896 reveal that they are novel GH31 and GH15 enzymes, respectively. Kfla1895 effectively hydrolyzes  $\alpha$ -(1 $\rightarrow$ 3)-glucosidic linkages in both CNN and  $\alpha$ -isomaltosyl-(1 $\rightarrow$ 3)- $\alpha$ -isomaltose, but the hydrolyzing activities with other substrates having an  $\alpha$ -isomaltosyl moiety (isomaltotriose) or an  $\alpha$ -(1 $\rightarrow$ 3)-glucosidic linkage

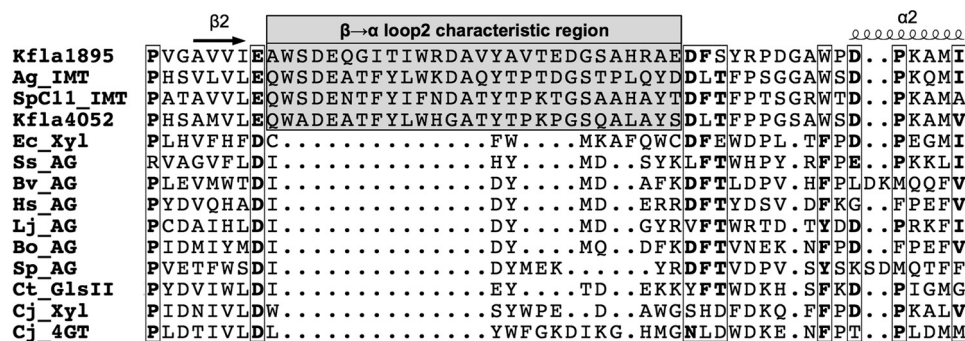


FIGURE 6. **Characteristic sequence feature of Kfla1895 and IMT.** Multiple sequence alignment around  $\beta\rightarrow\alpha$  loop 2 in catalytic ( $\beta/\alpha$ )<sub>6</sub>-barrel domain of GH31. The secondary structure of *B. vulgaris*  $\alpha$ -glucosidase (16) is shown above the sequences. The enzyme abbreviations are the same as described in the legends to Figs. 3 and 5A.

(nigerose) were very low (Table 1). These results indicate that Kfla1895 has a strong preference for the  $\alpha$ -(1 $\rightarrow$ 3)-isomaltosyl moiety and effectively hydrolyzes the  $\alpha$ -(1 $\rightarrow$ 3)-glucosidic linkage, and thus should be termed 1,3- $\alpha$ -isomaltosidase. GH31 contains glycoside hydrolases having different substrate specificity, including  $\alpha$ -glucosidase (16),  $\alpha$ -xylosidase (17), and  $\alpha$ -galactosidase (18), but their reactions share a common feature, liberation of a monosaccharide. Kfla1895 is the only GH31 enzyme to liberate a disaccharide. This difference in product specificities should be attributable to a difference in the structures of their active sites. All GH31 enzymes of known structure have a pocket-shaped active site that is occupied by a monosaccharide moiety at the non-reducing end of the substrate (16). In contrast, it is speculated that Kfla1895 possesses a deep pocket-shaped or groove-shaped active site that accommodates an isomaltosyl moiety. Furthermore, Kfla4052 is expected to have an active-site structure similar to that of Kfla1895 because this enzyme also recognizes an isomaltosyl moiety in its transferring reaction. The sequence comparison suggests that Kfla1895 and all IMTs possess a characteristic region at the loop joining  $\beta$ -strand 2 to  $\alpha$ -helix 2 in the catalytic ( $\beta/\alpha$ )<sub>6</sub>-barrel domain (Fig. 6). Such loop forms part of the rim of the active-site pocket in the structure-known GH31 enzymes. The characteristic region of Kfla1895 and IMTs in  $\beta\rightarrow\alpha$  loop 2 might contribute to their unique substrate recognition.

The enzymatic properties of Kfla1896 are also novel. Kfla1896 displays strict substrate specificity for isomaltose (Tables 1 and 2). This specificity is similar to that of oligo-1,6-glucosidase (EC 3.2.1.10), which belongs to GH13 (19). However, their reaction mechanisms are different (20). Oligo-1,6-glucosidase follows a double-displacement mechanism, which achieves the hydrolysis of a glucoside with net retention of anomeric configuration. However, GH15 enzymes, including Kfla1896, achieve catalysis using a single-displacement mechanism, which is performed with net inversion. Thus Kfla1896 should be distinguished from oligo-1,6-glucosidase and be termed isomaltose glucohydrolase. The substrate specificity of Kfla1896 is unique among members of GH15. Almost all of the enzymes classified into GH15 are glucoamylases (EC 3.2.1.3), which generally display high substrate specificity for soluble starch. Some bacterial glucoamylases, however, prefer malto-oligosaccharides to soluble starch (14, 21, 22), and only two enzymes, glucodextranase (23) and  $\alpha,\alpha$ -trehalase (24), are

known to have different substrate specificities. The glucodextranase derived from *A. globiformis* I42 displays 100- and 19-fold higher activity for dextran and isomaltose, respectively, than for soluble starch (22). Kfla1896 and this glucodextranase have the same regioselectivity for  $\alpha$ -1,6-glucosidic linkages but a different preference for the degree of polymerization of their substrates. Mizuno *et al.* (23) proposed that Gln<sup>380</sup> and Trp<sup>582</sup> contributed to the regioselectivity of the glucodextranase. However, their equivalent residues in Kfla1896 were unclear because these enzymes share low sequence similarity. Many GH15 enzymes have some additional domains, such as starch-binding domain of fungal enzymes and a unknown function N-terminal  $\beta$ -sandwich domain of bacterial enzymes, to the catalytic ( $\alpha/\alpha$ )<sub>6</sub>-barrel domain (26), but Kfla1896 is predicted to have only the ( $\alpha/\alpha$ )<sub>6</sub>-barrel domain. It is likely that the strict specificity of Kfla1896 for isomaltose is achieved by the catalytic domain and does not require such additional domains, which generally interact with long-chain substrates at a distance from the active site. Kfla1896 may possess an active-site structure that is different from those of the GH15 enzymes of known structure. Its unique substrate recognition mechanisms can be revealed through other means, like crystal structure analysis.

In conclusion, we elucidated a starch utilization pathway that proceeds via CNN in *K. flavida*. The intracellular degradation of CNN was catalyzed by two novel glycoside hydrolases, a 1,3- $\alpha$ -isomaltosidase (Kfla1895) of GH31 and an isomaltose glucohydrolase (Kfla1896) of GH15. The identification of the enzymes will expand our understanding of structure-function relationships among glycoside hydrolases.

## Experimental Procedures

**CNN Production and Carbohydrate Utilization by *K. flavida***—*K. flavida* NBRC 14399<sup>T</sup> was obtained from the Biological Resource Center, National Institute of Technology and Evaluation (Tokyo, Japan). The cells were revived and grown on yeast extract/malt extract (0.4% Bacto yeast extract, 1% Bacto malt extract, and 0.4% glucose) agar according to the protocol supplied with the organism. Liquid yeast extract/malt extract medium was inoculated with a single colony and cultured at 30 °C for 72 h with shaking. The resultant seed culture was diluted 20-fold with CNN-producing medium (0.1% Bacto yeast extract, 0.2% Bacto peptone, 0.1% Bacto beef extract, 0.05% MgSO<sub>4</sub>·7H<sub>2</sub>O, and 5% soluble starch) and cultivated at

## Two Novel Glycosidases of GH31 and GH15 Degrade CNN

30 °C with shaking. Soluble starch was replaced by 5% glucose, maltose, or CNN as a sole carbon source for testing carbohydrate assimilation.

**Purification and Analysis of CNN**—The culture supernatant was obtained by centrifugation (4,500 × g, 10 min, 4 °C). Ethanol was added to the culture supernatant to a final concentration of 80% (v/v), and the resultant precipitate containing soluble starch was removed by centrifugation (12,000 × g, 10 min, 4 °C). The supernatant was dried with a rotary evaporator and the remaining material was redissolved in H<sub>2</sub>O. Residual maltooligosaccharides in the solution were eliminated by two-step treatment with glucoamylase (70 units/ml) from *Aspergillus niger* (Sigma) in 0.05 mM sodium acetate buffer (pH 5.0) at 50 °C for 20 h and a commercially available bakers' yeast. The yeast cells were removed by centrifugation (12,000 × g, 10 min, 4 °C), followed by filtration with a Minisart filter (pore size 0.2 μm; Sartorius Stedim Biotech, Goettingen, Germany). The filtrate was desalted using Amberlite MB-4 (Organo Corporation, Tokyo, Japan), concentrated *in vacuo*, and subjected to preparative HPLC using a Tosoh HPLC system (Tokyo, Japan) equipped with a Cosmosil Sugar-D column (φ 10 × 250 mm; Nacalai Tesque, Kyoto, Japan). The sugars were eluted with an isocratic mobile phase of 70% (v/v) acetonitrile at a flow rate of 3 ml/min. The fractions containing only CNN were identified using TLC as described below.

The structure of the purified CNN was confirmed by ESI-MS analysis using an Exactive mass spectrometer (Thermo Fisher Scientific; Waltham, MA) and NMR analysis using a Bruker AMX500 (<sup>1</sup>H, 500 MHz; <sup>13</sup>C, 126 MHz) spectrometer (Bruker, Billerica, MA). The concentration of the purified CNN was determined using the phenol-sulfuric acid method (27) with glucose as a standard. The concentration of CNN in the culture supernatant was determined using a high-performance anion exchange chromatography system equipped with a pulsed amperometric detector and a CarboPac PA1 column (φ 4 × 250 mm; Dionex, Sunnyvale, CA). The solution obtained prior to the elimination of maltooligosaccharides was subjected to the analysis. The sugars were eluted with an isocratic mobile phase of 0.8 M NaOH at a flow rate of 0.8 ml/min. Sorbitol (100 μM) was used as an internal standard. TLC was performed using a Silica Gel 60 aluminum plate (Merck Millipore, Darmstadt, Germany). Carbohydrates were developed twice using a solvent system of acetonitrile/H<sub>2</sub>O (75:25; v/v), and visualized by heating with a reagent containing 0.03% 1-naphthol and 5% sulfuric acid in methanol.

**CNN-degrading Activity of *K. flavida***—*K. flavida* cells (A<sub>600</sub> = 30) cultured using CNN-producing medium were disrupted with a mortar and pestle in liquid nitrogen and suspended in 1 ml of 20 mM HEPES-NaOH (pH 7.5). A portion of the suspension (500 μl) was vortexed well and centrifuged (13,700 × g, 10 min, 4 °C). The resultant supernatant was isolated as a cell-free lysate, and the precipitate was re-suspended in 500 μl of 20 mM HEPES-NaOH (pH 7.5) as a membrane fraction. The cell-free lysate or the membrane fraction (190 μl) was mixed with 100 mM CNN (10 μl) and incubated at 30 °C for 24 h. These reaction mixtures were analyzed using TLC.

**Semiquantitative RT-PCR**—Total RNA from *K. flavida* cells cultured in CNN-producing medium was isolated using the NucleoSpin RNA kit (Takara Bio, Kusatsu, Japan). Each total

RNA sample (200 ng) was subjected to reverse transcription using PrimeScript reverse transcriptase with random 6-mer oligonucleotide primers (PrimeScript RT-PCR Kit; Takara Bio). The resultant reaction mixtures (1 μl) were used as templates for subsequent PCR. TaKaRa Ex TaqHS DNA polymerase (Takara Bio) was used in assays to detect mRNA encoding *Kfla\_4051*, *Kfla\_4052*, *Kfla\_1895*, *Kfla\_R0040*, and TaKaRa Ex TaqDNA polymerase (Takara Bio) was used in assays to detect mRNA encoding *Kfla\_1896*. The oligonucleotide primers used for the PCR were as follows: 5'-CCTTACCTGACGCTGAGGAG-3' and 5'-CCGGTACGGCTACCTTGTTA-3' for *Kfla\_R0040* (775 bp), 5'-GCGCAGTACAAGAACACCAA-3' and 5'-GTAGTACGGCGTGAGCTCGT-3' for *Kfla\_4051* (783 bp), 5'-CGAGATGCTCGACCAGTACA-3' and 5'-TACCACCA-CGACTGAACAGC-3' for *Kfla\_4052* (758 bp), 5'-CGGTGGTCTTCGAGCAGTA-3' and 5'-GAAGTGCTCGACCAGGT-AGC-3' for *Kfla\_1895* (776 bp), and 5'-TACGGCATGTGGC-TGTGGTC-3' and 5'-GTCGGCGAGGATCAGGTA-3' for *Kfla\_1896* (723 bp). The numbers in parentheses indicate the sizes of their amplified DNA fragments. The PCR mixtures supplemented with 1× Loading Buffer (Takara Bio) (7 μl total volume) were subjected to agarose gel electrophoresis, and the amplified DNA fragments were detected with ethidium bromide under a UV lamp.

**Cloning and Construction of Expression Plasmid**—The genome DNA of *K. flavida* was isolated using the DNeasy Blood & Tissue Kit (Qiagen, Hilden, Germany). Open reading frames were amplified by PCR from the genomic DNA using the following primers: 5'-GTAAACGCGTGCTGAAGGTGGTC-CAC-3' and 5'-ATCTTGGCAGCCGGTGACCCAA-3' for *Kfla\_4051*, 5'-GCAGACAAGTGAGGCTGTAG-3' and 5'-GATCAGCAGCACGAAGGCCATC-3' for *Kfla\_4052*, 5'-ACGGCATGTACCTGATCCTC-3' and 5'-ACAATAGGCG-AGGCGTACC-3' for *Kfla\_1895*, and 5'-AGACCAAGGTCA-ACGGTCTG-3' and 5'-GCGTACGGGTGCTCGATA-3' for *Kfla\_1896*. PCR was performed by using KOD-Plus-DNA polymerase or KOD FX Neo DNA polymerase (Toyobo, Osaka, Japan). Each PCR product was ligated into the EcoRV site of the plasmid pBluescript II SK(+) (Agilent Technologies, La Jolla, CA) using Ligation Kit version 2 (Takara Bio), and the resulting plasmids were propagated in *E. coli* DH5α. The sequences were analyzed by FASMAC Co., Ltd. (Atsugi, Japan).

The proteins encoded by the genes designated *Kfla4051*, *Kfla4052*, *Kfla1895*, and *Kfla1896* were heterologously expressed in *E. coli* as N-terminal His<sub>6</sub> tag fusion proteins. DNAs encoding the putative mature regions of *Kfla4051* (Val<sup>25</sup>-Phe<sup>948</sup>), *Kfla4052* (Gly<sup>39</sup>-Pro<sup>1108</sup>), *Kfla1895* (Met<sup>1</sup>-Ser<sup>723</sup>), or *Kfla1896* (Met<sup>1</sup>-Ala<sup>385</sup>), which were predicted using the SignalP 4.1 server (28), were amplified by PCR using PrimeSTAR HS (Takara Bio) or KOD-plus-Neo (Toyobo) DNA polymerase and the pairs of primers containing NdeI or HindIII sites (underlined) as follows: 5'-AAACATATGTTGGTGCA-GAGGGTCCAGTT-3' and 5'-TTTAAGCTTTCAGAAGCC-GCCGGTCGTC-3' for *Kfla\_4051*, 5'-AAACATATGGGCA-CGCTGACGGGCGTCTT-3' and 5'-TTTAAGCTTTCATG-GGCGTGCCACCGTGA-3' for *Kfla\_4052*, 5'-AAACATAT-GATCAAGCACCGCCCGCACG-3' and 5'-TTTAAGCTTTCAGCTGAAGACGGGCTGC-3' for *Kfla\_1895*, and 5'-AAA-

CATATGACCACCTCCGCCCGGGACA-3' and 5'-TTTAA-GCTTTCAGGCGTCCTTGGCGGC-3' for *Kfla\_1896*. Each PCR product was digested with NdeI and HindIII and inserted between the NdeI and HindIII sites of plasmid vector pET-28a (Merck Millipore).

The site-directed mutations were performed with PCR using PrimeSTAR mutagenesis basal kit (Takara Bio). The primers, of which underlined nucleotides indicates the mutated codons, are as follows: 5'-AAGACCGCGGGCGGCGAGCACGCC-TGG-3' and 5'-GCCGCCCGCGGTCTTGAATCCGTC-GAC-3' for *Kfla1895* Asp<sup>451</sup> → Ala mutation, 5'-GCCGGCG-CGGAGGACTCCACCTGGCAG-3' and 5'-GTCTCCGCG-CGGGCCAGAAAGATGCC-3' for *Kfla1895* Asp<sup>516</sup> → Ala mutation, 5'-TGGTGGGCGGAGCACGTCGAGCATCGG-3' and 5'-GTGCTCCGCCACCAGTCGTAGCAAGG-3' for *Kfla1896* Glu<sup>178</sup> → Ala mutation, and 5'-CTGCCGGCGCAG-GTCCCGCACCATCTG-3' and 5'-GACCTGCGCCGG-CAGGTCACCGTCGGC-3' for *Kfla1896* Glu<sup>335</sup> → Ala mutation.

**Production, Purification, and Characterization of *Kfla4052***—*E. coli* Rosetta (DE3) cells (Merck Millipore) were transformed with the pET-28a plasmid harboring the *Kfla4052* gene. A transformant was cultured overnight at 30 °C in LB medium (1% Bacto tryptone, 0.5% Bacto yeast extract, and 0.5% NaCl) containing 50 mg/liter of kanamycin and 30 mg/liter of chloramphenicol. The resultant seed culture was diluted 20-fold with TB medium (1.2% Bacto tryptone, 2.4% Bacto yeast extract, 0.4% (v/v) glycerol, 170 mM KH<sub>2</sub>PO<sub>4</sub>, and 720 mM K<sub>2</sub>HPO<sub>4</sub>, pH 7.2) supplemented with 50 mg/liter of kanamycin, and growth was continued at 37 °C. When the A<sub>600</sub> reached 0.5–0.7, the culture broth was cooled on ice for 30 min, and then protein expression was induced by the addition of isopropyl β-D-thiogalactopyranoside (1 mM). Expression was allowed to continue at 12 °C for 24 h. The cells were harvested by centrifugation (12,000 × g, 10 min, 4 °C), suspended in Buffer-A (20 mM sodium phosphate buffer (pH 7.5) and 0.3 M NaCl) supplemented with 0.1% Triton X-100 and 5% (v/v) glycerol, and disrupted by sonication. The cell-free lysate obtained by centrifugation (12,000 × g, 10 min, 4 °C) was applied to a Ni-chelating Sepharose Fast Flow column (GE Healthcare, Buckinghamshire, England). After the column was washed with 20 mM imidazole in Buffer A, the adsorbed proteins were eluted with 500 mM imidazole in Buffer A. The active fractions were dialyzed against Buffer B (20 mM sodium acetate buffer (pH 5.5)) and then loaded onto a Resource S column (6 ml; GE Healthcare). After the column was washed with 0.3 M NaCl in Buffer B, the adsorbed proteins were eluted with a linear gradient of 0.3 to 1 M NaCl in Buffer B. Electrophoretically homogeneous *Kfla4052* was dialyzed against Buffer B and concentrated using a Vivaspin 20–50K (GE Healthcare). The concentration of the purified *Kfla4052* was determined using its absorbance at 280 nm and the theoretical extinction coefficient (216,010 M<sup>-1</sup> cm<sup>-1</sup>) calculated using ProtParam server (29).

*Kfla4052* activity was measured at 37 °C in a standard reaction mixture containing 40 mM MES-NaOH (pH 6.5), 1 mM CaCl<sub>2</sub>, 10 mM panose, and *Kfla4052*, which was diluted to an appropriate concentration using 20 mM MES-NaOH (pH 6.5) containing 0.3% Triton X-100. The reaction mixture (50 μl)

was collected at 10 min and the reaction was stopped by treatment at 100 °C for 1 min. The solution was diluted 3-fold with 2 M Tris-HCl (pH 7.0), and the concentration of glucose was measured using a mutarotase-glucose oxidase method (30). One unit of *Kfla4052* was defined as the amount of enzyme that liberates 1 μmol of glucose/min from panose under the standard reaction conditions.

The effect of pH on the activity was investigated under the standard assay conditions but using 40 mM sodium acetate buffer (pH 3.5, 4.5, and 5.4), 40 mM MES-NaOH (pH 6.0 and 6.5), 20 mM MOPS-NaOH (pH 7.0 and 7.7), 20 mM HEPES-NaOH (pH 8.2 and 8.5), or 40 mM glycine-NaOH (pH 9.0 and 10.0). For measurements of pH stability, *Kfla4052* was incubated in 0.3% Triton X-100 and 20 mM glycine-HCl (pH 2.4 and 3.2), sodium acetate buffer (pH 3.9, 4.5, and 5.3), MES-NaOH (pH 6.0), MOPS-NaOH (pH 7.1), HEPES-NaOH (pH 7.9), glycine-NaOH (pH 9.1 and 10.1), or CAPS-NaOH (pH 11.1, 11.4, and 11.8) buffer at 4 °C for 24 h. Residual activity was measured under standard assay conditions. For thermostability measurements, *Kfla4052* was kept at 30–70 °C for 15 min, and then its residual activity was measured under standard assay conditions. The stable region was defined as the pH or temperature range exhibiting residual activity of more than 90%.

**Production and Purification of *Kfla1895*, *Kfla1896*, and Their Mutant Enzymes**—*E. coli* Rosetta (DE3) cells were transformed with pET-28a plasmids harboring the *Kfla1895* gene, the *Kfla1896* gene, or their mutant gene. The production procedures were the same as those used to produce *Kfla4052*, except that their inductions were performed by adding 0.1 mM isopropyl β-D-thiogalactopyranoside in LB medium at 20 °C for 6–16 h. The enzymes were purified with a nickel chelating Sepharose column using Buffer C (20 mM sodium phosphate buffer (pH 7.0) and 0.3 M NaCl) as a basal buffer. Electrophoretically homogeneous *Kfla1895*, *Kfla1896*, or their mutant was dialyzed against 20 mM sodium phosphate buffer (pH 7.0 or 8.0, respectively) and concentrated using Vivaspin 20–50K or –30K. The concentrations of the purified enzymes were determined using their absorbances at 280 nm and theoretical extinction coefficients, calculated using ProtParam server, of 192,280 and 112,410 M<sup>-1</sup> cm<sup>-1</sup>, respectively.

**Characterization of *Kfla1895*, *Kfla1896*, and Their Mutants**—*Kfla1895* activity was measured at 35 °C in a standard reaction mixture containing 80 mM sodium phosphate buffer (pH 8.0), 2 mM CNN, and *Kfla1895* and its derivatives, which were diluted to an appropriate concentration using 20 mM sodium phosphate buffer (pH 7.0) containing 0.1% Triton X-100. Reaction mixtures (50 μl) were collected at 3 and 10 min, and the reactions were stopped by treatment at 80 °C for 2 min. The solution was diluted 10-fold with H<sub>2</sub>O, and the concentration of reducing sugar was measured using the 2,2'-biconchinate method (31) with glucose as the standard. One unit of *Kfla1895* was defined as the amount of enzyme that liberates 1 μmol of reducing sugar/min from CNN under the standard reaction conditions.

*Kfla1896* activity was measured at 35 °C in a standard reaction mixture containing 40 mM sodium acetate buffer (pH 6.0), 2 mM isomaltose, and *Kfla1896* and its derivatives, which were diluted to an appropriate concentration using 20 mM sodium phosphate buffer (pH 8.0) containing 0.1% Triton X-100. The

## Two Novel Glycosidases of GH31 and GH15 Degrade CNN

reaction was stopped at 10 min by 3-fold dilution with 2 M Tris-HCl (pH 7.0), and the concentration of glucose was measured using the mutarotase-glucose oxidase method. One unit of Kfla1896 was defined as the amount of enzyme that hydrolyzed 1  $\mu$ mol of isomaltose per min under standard reaction conditions.

The effect of pH (from pH 2.6 to 10.3) on enzymatic activity was investigated under standard assay conditions, except using Britton-Robinson buffer (a mixture of 40 mM acetic acid, 40 mM phosphoric acid, and 40 mM boric acid adjusted to the appropriate pH with 0.2 N NaOH) as the reaction buffer. To measure pH stability, Kfla1895 or Kfla1896 was incubated in 10-fold-diluted Britton-Robinson buffer (pH 3.1 to 11.2) at 4 °C for 24 h, and then its residual activity was measured under standard assay conditions. To measure thermostability, Kfla1895 or Kfla1896 were kept at 25 °C–55 °C for 15 min, and then its residual activity was measured under standard assay conditions. The stable region was defined as the pH or temperature range exhibiting residual activity of more than 90%.

Substrate specificity was analyzed by measuring the initial rates of hydrolysis of various substrates under standard reaction conditions. Potential Kfla1895 substrates, tested at 10 mM concentration, included CNN, isomaltotriose, panose, and nigerose. Potential Kfla1896 substrates included isomaltose, isomaltotriose, panose, maltose, kojibiose, nigerose, trehalose, and CNN at 10 mM concentrations, as well as 2 mg/ml of dextran 10 and soluble starch. For both enzymes, initial reaction rates with CNN and the others were determined using the rate of the increase in reducing sugar content and glucose, respectively.

The kinetic parameters,  $k_{\text{cat}}$  and  $K_m$ , for substrate hydrolysis were calculated from  $s$ - $v$  plots by fitting to the Michaelis-Menten equation using KaleidaGraph 3.6J software (Synergy Software, Reading, PA). The substrate concentrations were 2–40 mM CNN for Kfla1895 and 1–20 mM isomaltose, isomaltotriose, and panose for Kfla1896. Because the  $K_m$  value of Kfla1895 for panose was so large, only the  $k_{\text{cat}}/K_m$  value was determined from the Lineweaver-Burk plots at concentrations from 1.7 to 10 mM. Each measurement was made in triplicate.

The anomeric form of the product resulting from Kfla1896-catalyzed hydrolysis was determined by using 4-nitrophenyl  $\alpha$ -glucopyranoside as a substrate. The enzyme (1.8 units/ml) was incubated with 7.5 mM 4-nitrophenyl  $\alpha$ -glucopyranoside in 5 mM sodium phosphate buffer (pH 8.0) at 30 °C for 20 min. The anomeric form of glucose produced by the reaction was analyzed by HPLC using a previous report procedure (32).

**Author Contributions**—T. T. and M. O. designed the research and generated the manuscript. E. M. characterized Kfla4052 and J. S. performed the experiments shown in Fig. 2. T. T. performed all other experiments. T. I. and A. K. provided technical assistance and contributed to the preparation of the figures. All authors reviewed the results and approved the final version of the manuscript.

**Acknowledgments**—We thank Dr. E. Fukushi and Y. Takata of the GC-MS & NMR laboratory, Hokkaido University, for the NMR analysis, and T. Hirose of the Instrumental Analysis Services, the Global Facility Center, Hokkaido University for the ESI-MS analysis. We are grateful to Hayashibara Co. Ltd. (Okayama, Japan) for giving us purified CNN.

## References

1. Côté, G. L., and Biely, P. (1994) Enzymically produced cyclic  $\alpha$ -1,3-linked and  $\alpha$ -1,6-linked oligosaccharides of D-glucose. *Eur. J. Biochem.* **226**, 641–648
2. Nishimoto, T., Aga, H., Mukai, K., Hashimoto, T., Watanabe, H., Kubota, M., Fukuda, S., Kurimoto, M., and Tsujisaka, Y. (2002) Purification and characterization of glucosyltransferase and glucanotransferase involved in the production of cyclic tetrasaccharide in *Bacillus globisporus* C11. *Biosci. Biotechnol. Biochem.* **66**, 1806–1818
3. Aga, H., Nishimoto, T., Kuniyoshi, M., Maruta, K., Yamashita, H., Higashiyama, T., Nakada, T., Kubota, M., Fukuda, S., Kurimoto, M., and Tsujisaka, Y. (2003) 6- $\alpha$ -Glucosyltransferase and 3- $\alpha$ -isomaltosyltransferase from *Bacillus globisporus* N75. *J. Biosci. Bioeng.* **95**, 215–224
4. Mukai, K., Maruta, K., Satouchi, K., Kubota, M., Fukuda, S., Kurimoto, M., and Tsujisaka, Y. (2004) Cyclic tetrasaccharide-synthesizing enzymes from *Arthrobacter globiformis* A19. *Biosci. Biotechnol. Biochem.* **68**, 2529–2540
5. Côté, G. L., and Ahlgren, J. A. (2001) The hydrolytic and transferase action of alternanase on oligosaccharides. *Carbohydr. Res.* **332**, 373–379
6. Kim, Y. K., Kitaoka, M., Hayashi, K., Kim, C. H., and Côté, G. L. (2003) A synergistic reaction mechanism of a cycloalternan-forming enzyme and a D-glucosyltransferase for the production of cycloalternan in *Bacillus* sp. NRRL B-21195. *Carbohydr. Res.* **338**, 2213–2220
7. Aga, H., Maruta, K., Yamamoto, T., Kubota, M., Fukuda, S., Kurimoto, M., and Tsujisaka, Y. (2002) Cloning and sequencing of the genes encoding cyclic tetrasaccharide-synthesizing enzymes from *Bacillus globisporus* C11. *Biosci. Biotechnol. Biochem.* **66**, 1057–1068
8. Lombard, V., Golaconda Ramulu, H., Drula, E., Coutinho, P. M., and Henrissat, B. (2014) The carbohydrate-active enzymes database (CAZy) in 2013. *Nucleic Acids Res.* **42**, D490–495
9. Kim, Y. K., Kitaoka, M., Hayashi, K., Kim, C. H., and Côté, G. L. (2004) Purification and characterization of an intracellular cycloalternan-degrading enzyme from *Bacillus* sp. NRRL B-21195. *Carbohydr. Res.* **339**, 1179–1184
10. Hashimoto, Y., Yamamoto, T., Fujiwara, S., Takagi, M., and Imanaka, T. (2001) Extracellular synthesis, specific recognition, and intracellular degradation of cyclomalto-dextrins by the hyperthermophilic archaeon *Thermococcus* sp. strain B1001. *J. Bacteriol.* **183**, 5050–5057
11. Pukall, R., Lapidus, A., Glavina Del Rio, T., Copeland, A., Tice, H., Cheng, J. F., Lucas, S., Chen, F., Nolan, M., Labutti, K., Pati, A., Ivanova, N., Mavromatis, K., Mikhailova, N., Pitluck, S., Bruce, D., et al. (2010) Complete genome sequence of *Kribbella flavida* type strain (IFO 14399<sup>T</sup>). *Stand. Genomic Sci.* **2**, 186–193
12. Li, W., Cowley, A., Uludag, M., Gur, T., McWilliam, H., Squizzato, S., Park, Y. M., Buso, N., and Lopez, R. (2015) The EMBL-EBI bioinformatics web and programmatic tools framework. *Nucleic Acids Res.* **43**, W580–584
13. Okuyama, M., Okuno, A., Shimizu, N., Mori, H., Kimura, A., and Chiba, S. (2001) Carboxyl group of residue Asp647 as possible proton donor in catalytic reaction of  $\alpha$ -glucosidase from *Schizosaccharomyces pombe*. *Eur. J. Biochem.* **268**, 2270–2280
14. Coutinho, P. M., and Reilly, P. J. (1994) Structure-function relationships in the catalytic and starch binding domains of glucoamylase. *Protein Eng.* **7**, 393–400
15. Kazanov, M. D., Li, X., Gelfand, M. S., Osterman, A. L., and Rodionov, D. A. (2013) Functional diversification of ROK-family transcriptional regulators of sugar catabolism in the *Thermotogae* phylum. *Nucleic Acids Res.* **41**, 790–803
16. Tagami, T., Yamashita, K., Okuyama, M., Mori, H., Yao, M., and Kimura, A. (2015) Structural advantage of sugar beet  $\alpha$ -glucosidase to stabilize the Michaelis complex with long-chain substrate. *J. Biol. Chem.* **290**, 1796–1803
17. Okuyama, M., Mori, H., Chiba, S., and Kimura, A. (2004) Overexpression and characterization of two unknown proteins, YicI and YihQ, originated from *Escherichia coli*. *Protein Expr. Purif.* **37**, 170–179
18. Miyazaki, T., Ishizaki, Y., Ichikawa, M., Nishikawa, A., and Tonozuka, T. (2015) Structural and biochemical characterization of novel bacterial  $\alpha$ -galactosidases belonging to glycoside hydrolase family 31. *Biochem. J.* **469**, 145–158

19. Saburi, W., Mori, H., Saito, S., Okuyama, M., and Kimura, A. (2006) Structural elements in dextran glucosidase responsible for high specificity to long chain substrate. *Biochim. Biophys. Acta* **1764**, 688–698
20. McCarter, J. D., and Withers, S. G. (1994) Mechanisms of enzymatic glycoside hydrolysis. *Curr. Opin. Struct. Biol.* **4**, 885–892
21. Sauer, J., Sigurskjold, B. W., Christensen, U., Frandsen, T. P., Mirgorodskaya, E., Harrison, M., Roepstorff, P., and Svensson, B. (2000) Glucoamylase: structure/function relationships, and protein engineering. *Biochim. Biophys. Acta* **1543**, 275–293
22. Uotsu-Tomita, R., Tono-zuka, T., Sakai, H., and Sakano, Y. (2001) Novel glucoamylase-type enzymes from *Thermoactinomyces vulgaris* and *Methanococcus jannaschii* whose genes are found in the flanking region of the  $\alpha$ -amylase genes. *Appl. Microbiol. Biotechnol.* **56**, 465–473
23. Mizuno, M., Tono-zuka, T., Suzuki, S., Uotsu-Tomita, R., Kamitori, S., Nishikawa, A., and Sakano, Y. (2004) Structural insights into substrate specificity and function of glucodextranase. *J. Biol. Chem.* **279**, 10575–10583
24. Sakaguchi, M., Shimodaira, S., Ishida, S. N., Amemiya, M., Honda, S., Sugahara, Y., Oyama, F., and Kawakita, M. (2015) Identification of GH15 family thermophilic archaeal trehalases that function within a narrow acidic-pH range. *Appl. Environ. Microbiol.* **81**, 4920–4931
25. Robert, X., and Gouet, P. (2014) Deciphering key features in protein structures with the new ENDscript server. *Nucleic Acids Res.* **42**, W320–324
26. Marín-Navarro, J., and Polaina, J. (2011) Glucoamylases: structural and biotechnological aspects. *Appl. Microbiol. Biotechnol.* **89**, 1267–1273
27. Hodge, J. E., and Hofreiter, B. T. (1962) Determination of reducing sugars and carbohydrates. *Methods in Carbohydrate Chemistry* (Whistler, R. L., and Wolfrom, M. L., eds) Vol. 1, pp. 380–394, Academic Press, New York
28. Petersen, T. N., Brunak, S., von Heijne, G., and Nielsen, H. (2011) SignalP 4.0: discriminating signal peptides from transmembrane regions. *Nat. Methods* **8**, 785–786
29. Gasteiger, E., Hoogland, C., Gattiker, A., Duvaud, S., Wilkins, M. R., Appel, R. D., and Bairoch, A. (2005) Protein identification and analysis tools on the ExPASy server. *The proteomics Protocols Handbook* (Walker, J. M., ed) pp. 571–607, Human Press, New York
30. Miwa, I., Okudo, J., Maeda, K., and Okuda, G. (1972) Mutarotase effect on colorimetric determination of blood glucose with D-glucose oxidase. *Clin. Chim. Acta* **37**, 538–540
31. McFeeters, R. F. (1980) A manual method for reducing sugar determinations with 2,2'-bicinchoninate reagent. *Anal. Biochem.* **103**, 302–306
32. Kitamura, M., Okuyama, M., Tanzawa, F., Mori, H., Kitago, Y., Watanabe, N., Kimura, A., Tanaka, I., and Yao, M. (2008) Structural and functional analysis of a glycoside hydrolase family 97 enzyme from *Bacteroides thetaiotaomicron*. *J. Biol. Chem.* **283**, 36328–36337
33. Papadopoulos, J. S., and Agarwala, R. (2007) COBALT: constraint-based alignment tool for multiple protein sequences. *Bioinformatics* **23**, 1073–1079

## Two Novel Glycoside Hydrolases Responsible for the Catabolism of Cyclobis-(1→6)- $\alpha$ -nigerosyl

Takayoshi Tagami, Eri Miyano, Juri Sadahiro, Masayuki Okuyama, Tomohito Iwasaki and Atsuo Kimura

*J. Biol. Chem.* 2016, 291:16438-16447.

doi: 10.1074/jbc.M116.727305 originally published online June 14, 2016

---

Access the most updated version of this article at doi: [10.1074/jbc.M116.727305](https://doi.org/10.1074/jbc.M116.727305)

### Alerts:

- [When this article is cited](#)
- [When a correction for this article is posted](#)

[Click here](#) to choose from all of JBC's e-mail alerts

This article cites 32 references, 6 of which can be accessed free at <http://www.jbc.org/content/291/32/16438.full.html#ref-list-1>